

UNISENSORY INTRA-ROW NAVIGATION STRATEGY FOR ORCHARDS ENVIRONMENTS BASED ON SENSOR LASER

RANDERSON A. DE LEMOS*, LUCAS A. C. DE O. NOGUEIRA*, ALEXANDRE M. RIBEIRO*, LUIZ G. B. MIRISOLA†, MAURO F. KOYAMA‡, ELY C. DE PAIVA*, SAMUEL S. BUENO‡

**Faculdade de Engenharia Mecânica (FEM) da Universidade Estadual de Campinas (UNICAMP)
Rua Mendenleyv, 200, Cidade Universitária, 13083-860
Campinas, São Paulo, Brasil*

†*Divisão de Ciência da Computação (IEC) do Instituto Tecnológico de Aeronáutica (ITA)
Praça Marechal Eduardo Gomes, 50, 12228-900
São José dos Campos, São Paulo, Brasil*

‡*Centro de Tecnologia da Informação Renato Archer (CTI)
Rod. D. Pedro I (SP-65) - km.143.6, 13069-901
Campinas, São Paulo, Brasil*

Emails: randerson.lemos@gmail.com, lucas.nogueira@fem.unicamp.br,
amribeiro@fem.unicamp.br, lgm@ita.br, mauro.koyama@cti.gov.br,
elypaiva@fem.unicamp.br, samuel.bueno@cti.gov.br

Abstract— This work presents an unisensory autonomous navigation strategy for orchards environment using information provided by a single Light Detection and Ranging (LIDAR) sensor. A reference path is obtained with the use of the Random Samples and Consensus (RANSAC) method and an improvement is achieved using the Extended Kalman Filter (EKF). This path is used as the reference for a trajectory controller to guide the platform between the plantation corridor. The control strategy considers a proportional-integral controller actuating upon a given “look ahead error” composed of a lateral distance error plus a predict error which is an estimation of the lateral error evolution. Implementation codes are made available and a validation experiment is performed.

Keywords— Orchards, Laser LIDAR, Unisensory, RANSAC, EKF.

Resumo— O presente trabalho apresenta uma estratégia unisensorial de navegação autônoma para ambientes de cultivos que usa as informações de um único sensor de Detecção de Luz e Medida de Distância (LIDAR). Um caminho de referência é obtido a partir do uso do algoritmo de Consenso de Amostra Aleatória (RANSAC) e uma melhoria é alcançada utilizando o Filtro de Kalman Estendido (EKF). Esse caminho é usado como referência em um controle de trajetória responsável por guiar a plataforma por entre os corredores da plantação. A estratégia de controle considera um controlador proporcional-integral que atua sobre o erro de “distância projetada” composto pelo erro lateral acrescido por uma estimativa de sua evolução. Os códigos de implementação estão disponibilizados e um experimento de validação é realizado.

Palavras-chave— Cultivos, Laser LIDAR, Unissensorial, RANSAC, EKF.

1 Introduction

The number of agricultural applications for robotics is growing intensely in the last years. The recent advances of technologies and reduced cost of electronic devices have contributed to this growth. But, most importantly, it is the increasing demand from society for food, fuel and fiber that has been continuously pushing the agriculture sector for improvements and, as consequence, has opened space for new solutions such as robotics-based ones (Foley et al., 2011).

From the wide spectrum of agricultural problems addressed by robotics, one is related with the machinery automation for production improvement (de Lemos et al., 2017; Bechar and Vigneault, 2017; Thanpattranon et al., 2016; Bayar et al., 2015; Hiremath et al., 2014). For example, it was shown that autonomous farm vehicles increase the overall production efficiency of fruit orchards and reduce operator fatigue (Bergerman et al., 2015).

This paper addresses the problem of autonomous navigation between rows of cultivated species for a four-wheeled platform. It reports an unisensory intra-row navigation strategy where a LIDAR is the unique electronic device used for sensing the orchard surroundings. It also presents a validation of the unisensory strategy in a experiment where a four-wheeled platform autonomously goes through a corridor formed by the rows of the orchard shown in Figure 1.

The main contributions reported are:

- improvements of the filtering stage of the unisensory solution presented by de Lemos et al. (2017);
- experimental validation of the unisensory solution described in this manuscript;
- release of the solution in the form of open-source and ready-to-use code to the community.



Figure 1: Orchard where the validation experiment of the unisensory intra-row navigations strategy were performed.

This paper is organized as follows: Section 2 details the intra-row orchard navigation problem approached and the solution proposed. Section 3 describes the Trajectory Generation System and the filtering solution used. Section 4 describes the Control System and the control law used. Section 5 discusses the implementation details and the platform used in the validation experiment. Section 6 reports the results obtained and Section 7 presents conclusions.

2 Motivations

The intra-row navigation problem for orchards environment approached is mainly characterized by the static nature of planting layout, where the crops are aligned one after another, forming equally spaced rows. Nevertheless, this layout is subjected to variations in terms of displacement of the rows of the cultivated species, in the weather conditions, in the hardness of the ground, and in the daily illumination (de Lemos et al., 2017). Hence, the solutions proposed to solve it must be robust to such variations.

Other researches have studied this problem. Their solutions to deal with the randomness of the orchards environment usually consider a multisensory hardware architecture. For example, in papers presented by Thanpattranon et al. (2016) and Hiremath et al. (2014) this multisensory hardware architecture is considered. Although in minority proportion, solutions with unisensory hardware architecture are also found in the literature as in papers of de Lemos et al. (2017) and Bergerman et al. (2015).

The solution presented in this paper is based on an unisensory hardware architecture and it is the same as the one presented in the paper of de Lemos et al. (2017). Nevertheless the software architecture solution, in the algorithm level, is different and enhanced. More specifically, the filtering stage of the software was improved since now an EKF (Bar-Shalom et al., 2004) is used upon a non-linear system to better estimate the angular and linear coefficients of a reference path,

which passes through the center of the intra-row corridor and is used as reference by the control law to guide the platform (de Lemos et al., 2017).

The solution presented here is organized into two main systems: one responsible for providing a reference path, called the Trajectory Generation System, and the other responsible for guiding the platform towards the reference path, called the Control System.

3 Trajectory Generation System

The Trajectory Generation System is responsible for generating a reliable reference path for the Control System. The system considers only the information provided by a LIDAR as Figure 2 illustrates, where the salmon semi-circle is the sensor range and the blue marks are the data provided by it.

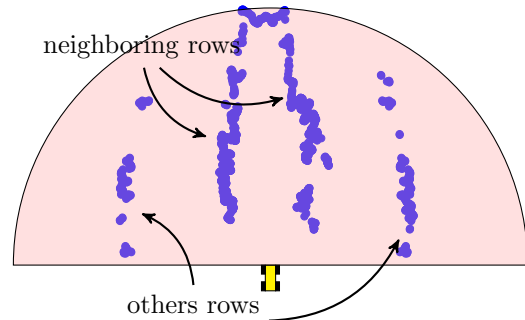


Figure 2: Rows orchard data from the LIDAR.

Due the characteristics of the orchards environment, the information provided by the sensor contains data from rows other than the ones neighboring the platform. As this data is unwanted, it is removed by the use of a window of interest. The window has a width w and a length l and eliminates all data that are outside its borders. The remaining data is split into two groups, one containing the data located at the left side and the other containing the data located at the right side of the platform. Next, a non-deterministic method for model adjustment, RANSAC (Fischler and Bolles, 1981), is applied and support lines that passes through the neighboring rows are obtained (de Lemos et al., 2017).

RANSAC adds robustness to the Trajectory Generation System against potential outliers (Zuliani, 2009) that might be present in the data. From the support lines, a bisector line is computed. This line is used along with the linear and angular velocities of the platform in the filtering stage to obtain a reference path. These steps and its results are synthesized in Figure 3.

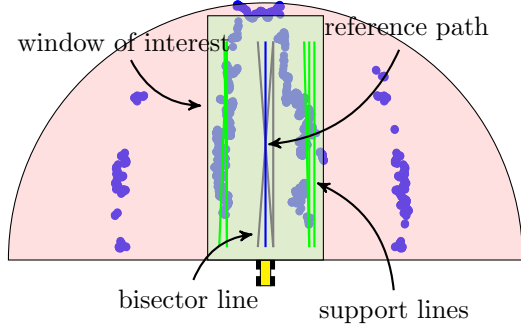


Figure 3: Steps and results synthesized of the Identification System.

Filtering Stage

At the algorithm level, the contributions reported are concentrated in the filtering stage of the Trajectory Generation System. In this stage, a less noisy bisector line, the reference path, is obtained by the use of the Extended Kalman Filter. The filter equations capture the relations between coefficients of the reference path and the kinematics of an Ackermann platform.

With the non-linear system framework

$$\begin{aligned} \mathbf{x}_k &= \mathbf{f}(\mathbf{x}_{k-1}) + \Gamma \boldsymbol{\xi}_{k-1} \\ \mathbf{y}_k &= \mathbf{h}(\mathbf{x}_k) + \mathbf{v}_k \end{aligned}, \quad (1)$$

the state-space vector used is

$$\mathbf{x}_k = [\theta_k \quad b_k \quad \omega_k \quad \alpha_k \quad v_k \quad a_k]^\top, \quad (2)$$

where θ_k is the angle between the x -axis of the platform's local frame and the reference path (the $\arctan(\cdot)$ of its angular coefficient); b_k is the distance along the y -axis of the platform's local frame and the reference path (its linear coefficient); ω_k is the platform's angular velocity; α_k is the platform's angular acceleration; v_k is the platform's linear velocity and a_k is the platform's linear acceleration. The non-linear difference equation used is

$$\mathbf{f}(\mathbf{x}_k) = [{}^1f_k \quad {}^2f_k \quad {}^3f_k \quad {}^4f_k \quad {}^5f_k \quad {}^6f_k]^\top, \quad (3)$$

where

$$\begin{aligned} {}^1f_k &= \theta_k - \Delta t \omega_k \\ {}^2f_k &= b_k + \Delta t^2 \omega_k v_k + \\ &\quad + \Delta t (v_k - b_k \omega_k) \tan(\theta_k - \Delta t \omega_k) \\ {}^3f_k &= \omega_k + \Delta t \alpha_k \\ {}^4f_k &= \alpha_k \\ {}^5f_k &= v_k + \Delta t a_k \\ {}^6f_k &= a_k \end{aligned}. \quad (4)$$

The process random-vector used is

$$\Gamma \boldsymbol{\xi}_k = \begin{bmatrix} 1 & 0 & 0 & 0 \\ 0 & 1 & 0 & 0 \\ 0 & 0 & 0 & 0 \\ 0 & 0 & 1 & 0 \\ 0 & 0 & 0 & 0 \\ 0 & 0 & 0 & 1 \end{bmatrix} \begin{bmatrix} {}^1\xi_k \\ {}^2\xi_k \\ {}^3\xi_k \\ {}^4\xi_k \end{bmatrix}, \quad (5)$$

where $\boldsymbol{\xi}_k$ is a Gaussian noise with zero mean and covariance matrix Q . The measurement model function used is

$$\mathbf{h}(\mathbf{x}_k) = \begin{bmatrix} 1 & 0 & 0 & 0 & 0 & 0 \\ 0 & 1 & 0 & 0 & 0 & 0 \\ 0 & 0 & 1 & 0 & 0 & 0 \\ 0 & 0 & 0 & 0 & 1 & 0 \end{bmatrix} \begin{bmatrix} \theta_k \\ b_k \\ \omega_k \\ \alpha_k \\ v_k \\ a_k \end{bmatrix}. \quad (6)$$

The measurement random-vector used is

$$\mathbf{v}_k = [{}^1v_k \quad {}^2v_k \quad {}^3v_k \quad {}^4v_k]^\top, \quad (7)$$

where \mathbf{v}_k is a Gaussian noise with zero mean and covariance matrix R . In the observation model

$$\begin{aligned} \mathbf{y}_k &= [{}^1y_k \quad {}^2y_k \quad {}^3y_k \quad {}^4y_k]^\top = \\ &= (\mathbf{h}(\mathbf{x}_k) + \mathbf{v}_k)^\top, \end{aligned} \quad (8)$$

1y_k is the angular and 2y_k is the linear coefficient of the bisector line and 3y_k is the angular and 4y_k is the linear commanded velocity of the platform, which is assumed to be close to the real velocity of the platform (Nogueira et al., 2018)

4 Control System

The Control System is responsible for guiding the platform along the reference path. The system counts with a simple control strategy already validated in the context of the AURORA project (Azinheira et al., 2000; Cordeiro et al., 2012). The strategy considers a proportional-integral controller actuating upon the look ahead error δ_r . The look ahead error δ_r is the composition of two others errors: one is the known lateral error δ ; and the other is the predict error δ_v , which quantify the expectation of evolution of the lateral error δ . The geometrical interpretation of these errors are shown in Figure 4. Hence the crude control law is

$$\mathbf{u}(t) = K_p \delta_r(t) + K_i \int_0^t \delta_r(\tau) d\tau, \quad (9)$$

where K_p and K_i are control gains. After some mathematical manipulation (de Lemos et al., 2017), the resulting control law

$$\mathbf{u}(t) = K_{p^*} \delta(t) + K_{i^*} \int_0^t \delta(\tau) d\tau + K_{v^*} v_\perp, \quad (10)$$

is achieved, where K_{p^*} is a proportional gain, K_{i^*} is an integral gain, K_{v^*} is a velocity gain and v_\perp is

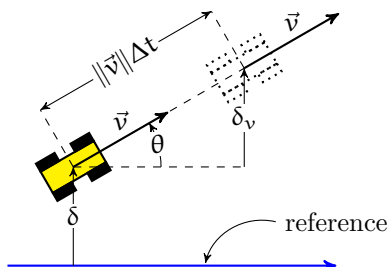


Figure 4: Geometric interpretation of the lateral error δ and the predict error δ_v .

the perpendicular velocity of the platform to the reference path. This is the actual control law used in the Control System.

A block diagram depicting the proposed trajectory generation and control system is shown in Figure 5. Its important to note LIDAR is the unique source of measured information and it feeds the EKF as well as the angular and linear commanded velocities. To overcome the dependency of the target velocity, it is acceptable to assume ω at instant k approximately equal to the velocity at instant $k - 1$, therefore a delayed structure is used.

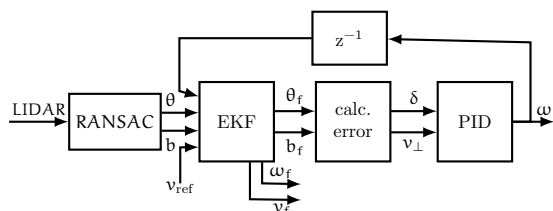


Figure 5: Overall system diagram.

The Kalman filter outputs are: θ_f , filtered angle; b_f , filtered linear coefficient; ω_f and v_f the estimated vehicle angular and linear velocities, respectively. The filtered coefficients are used to calculate the errors δ and v_{\perp} . Finally, the target angular velocity ω is obtained by the PID controller.

5 Implementation and Platform

All the intra-row navigation solution presented is implemented and ready-to-use. Its implementation were done under the Robot Operating System (ROS) (Quigley et al., 2009) framework and the source code, as a ROS package, is available at https://github.com/randersonLemos/ransac_corridor_control with a minimal documentation.

A four-wheeled platform, named Arqueiro Verde, developed in the context of the project VERDE (Nogueira et al., 2018) was used for the validation experiment. The platform, shown in Figure 6, has independent rear-traction with electronic differential and steering system similar to

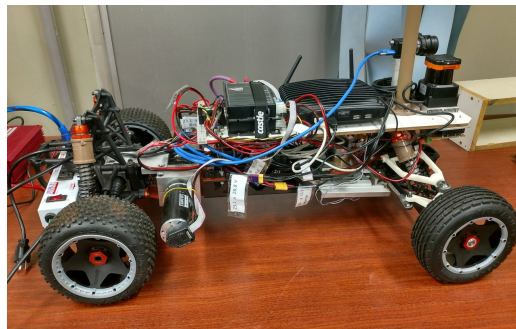


Figure 6: Four-wheeled platform for experiments Arqueiro Verde.

the Ackermann one. It is equipped with a collection of off-the-shelf sensors such as: global positioning system (GPS), inertial measurement unit (IMU), camera, LIDAR and others (Nogueira et al., 2018), remarking that only laser is used in this unisensory proposal.

6 Results

In the experimental validation stage of the unisensory solution, the values used in the covariance process matrix were

$$Q = \begin{bmatrix} 10.0 & 0.0 & 0.0 & 0.0 \\ 0.0 & 25.0 & 0.0 & 0.0 \\ 0.0 & 0.0 & 1.0 & 0.0 \\ 0.0 & 0.0 & 0.0 & 25.0 \end{bmatrix},$$

the values used in the covariance measurement matrix were

$$R = \begin{bmatrix} 20.0 & 0.0 & 0.0 & 0.0 \\ 0.0 & 100.0 & 0.0 & 0.0 \\ 0.0 & 0.0 & 2.0 & 0.0 \\ 0.0 & 0.0 & 0.0 & 10.0 \end{bmatrix},$$

and the values used in the control gains were

$$K_p^* = 0.1, \quad K_i^* = 0.001 \text{ and } K_v^* = 0.50.$$

All these values were adjusted following a trial and error experimental basis. The window of interest used had width $w = 10.0$ m and length $l = 10.0$ m and the target linear velocity of the platform was of $v = 1.0$ m/s. A sequence of results of the first thirty seconds of the experiment are shown. The vehicle is initially oriented toward the orchards rows, however, with an initial lateral error. It is expected a correction to accurately follow the center of the intra-row corridor.

In Figure 7, the evolution of the angular coefficient of the bisector line and of the reference path are shown. In Figure 8, the evolution of the linear coefficient of the bisector line and of the reference path are shown. One can note the effect of initial lateral error during the first 4 seconds.

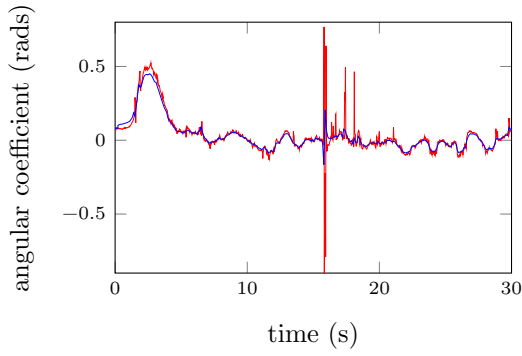


Figure 7: In red, the angular coefficient of the bisector line. In blue, the angular coefficient of the reference path.

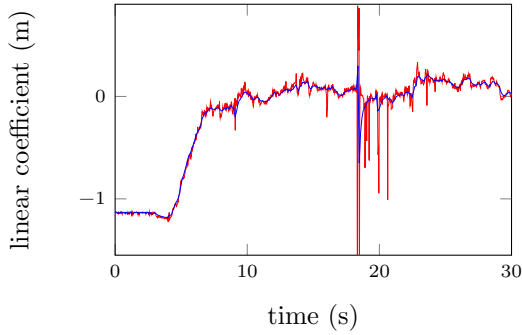


Figure 8: In red, the linear coefficient of the bisector line. In blue, the linear coefficient on the reference path.

Also, between 17s and 21s, the platform experienced a noisy LIDAR measurements due to irregularities on the ground. However both coefficients were properly filtered by EKF.

Figures 9 and 10 shows the evolution of the commanded and filtered angular and linear velocities, respectively. The step variations noted in the first 7 – 8 seconds are due to the large initial position error. The commanded velocities are a reflection of the trajectory generation system response in order to reach the center of the corridor.

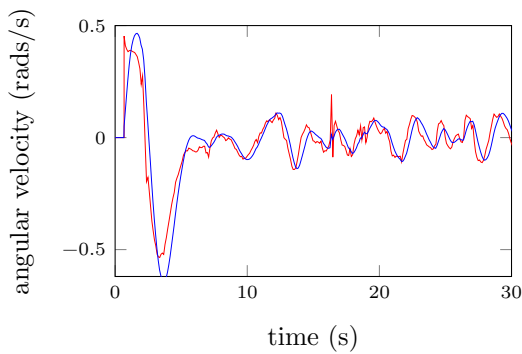


Figure 9: In red, the commanded angular velocity. In blue, the filtered angular velocity.

Figure 11 exposes qualitative informations of

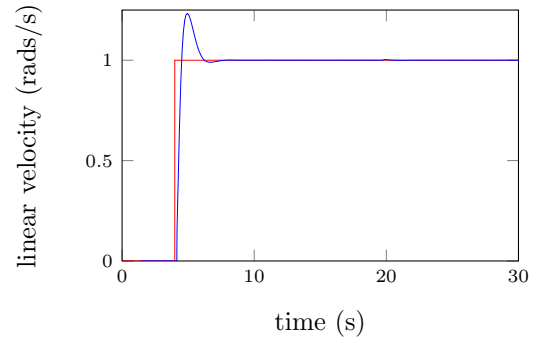


Figure 10: In red, the commanded linear velocity. In blue, the filtered linear velocity.

the experimental validation and gives an overall intuition of the unisensory solution behavior through a picture sequence of the platform traversing the orchard corridor autonomously. Here we highlight the initial vehicle pose (Figure 11a). Figure 12 shows a sequence of geometric in-

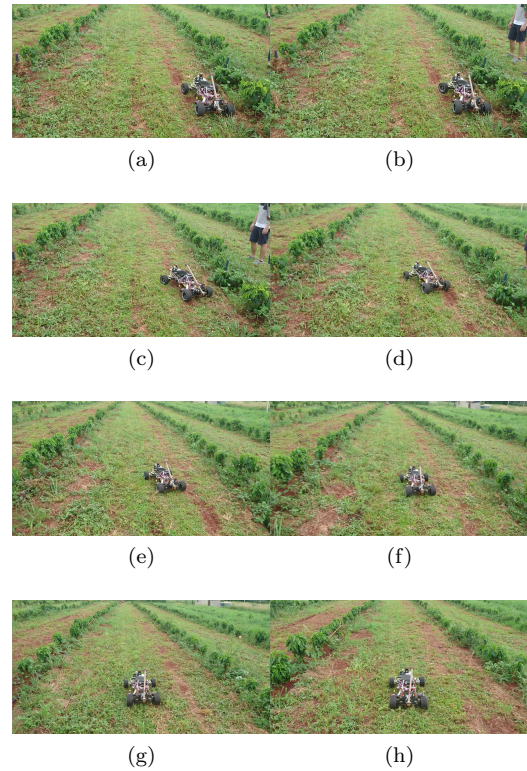
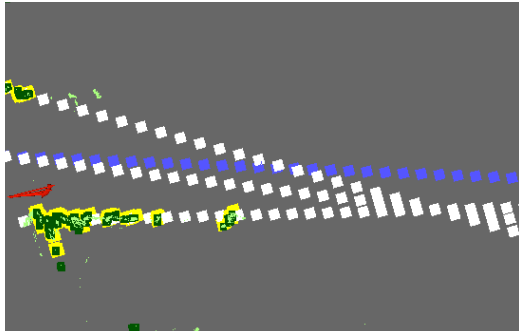


Figure 11: Platform in autonomous mode traversing the orchard corridor.

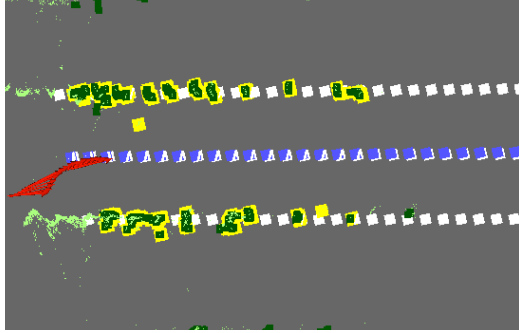
formation generated and used by the unisensory solution during the experimental validation. The platform pose is retrieved by the lidar odometry.

7 Conclusions

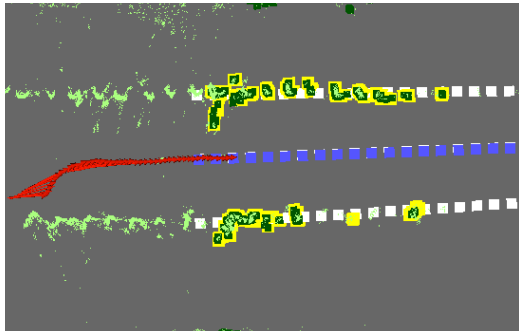
As the experimental results attest, the unisensory intra-row navigation strategy performed as expected. It successfully conducted the platform



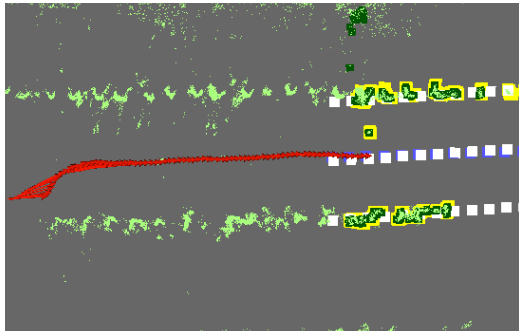
(a)



(b)



(c)



(d)

Figure 12: Geometric visualization of several informations generated during the validation experiment. In soft green, all point cloud generated by the laser LIDAR. In dark green, point cloud currently generated by the laser LIDAR. In yellow, point cloud used by method RANSAC. In white, support and bisector lines. In blue, reference path (filtered bisector line). In red, pose of the platform.

toward the orchard corridor at a linear velocity of 1.0 m/s. The trajectory generation system was able to properly detect the corridor lines. The filtering stage provided better and less noisy values of the reference path (filtered bisector line) ensuring a smooth controller action. The filtering stage was also able to provide consistent estimated values of the linear and angular velocities solely based on LIDAR sensor. In a future work the estimated velocities information can be used in other operation modules of the platform such as vehicle odometry and pose estimation.

8 Acknowledgment

The authors acknowledge the support of INCT - SAC - Sistemas Autônomos Colaborativos (CNPq. N. 465755/2014-3 and FAPESP N. 2014/50851-0), Regular FAPESP Auto_Verde (FAPESP N. 2018/04905-1) and Ph.D FAPESP (FAPESP N. 2018/05712-2).

References

- Azinheira, J. R., de Paiva, E. C., Ramos, J. and Bueno, S. (2000). Mission path following for an autonomous unmanned airship, *Robotics and Automation, 2000. Proceedings. ICRA'00. IEEE International Conference on*, Vol. 2, IEEE, pp. 1269–1275.
- Bar-Shalom, Y., Li, X. R. and Kirubarajan, T. (2004). *Estimation with applications to tracking and navigation: theory algorithms and software*, John Wiley & Sons.
- Bayar, G., Bergerman, M., Koku, A. B. and İlhan Konukseven, E. (2015). Localization and control of an autonomous orchard vehicle, *Computers and Electronics in Agriculture* **115**: 118–128.
- Bechar, A. and Vigneault, C. (2017). Agricultural robots for field operations. part 2: Operations and systems, *Biosystems Engineering* **153**: 110–128.
- Bergerman, M., Maeta, S. M., Zhang, J., Freitas, G. M., Hamner, B., Singh, S. and Kantor, G. (2015). Robot farmers: Autonomous orchard vehicles help tree fruit production, *IEEE Robotics & Automation Magazine* **22**(1): 54–63.
- Cordeiro, R. A., Azinheira, J. R., de Paiva, E. C. and Bueno, S. S. (2012). Efeitos da dinâmica tridimensional no controle de trajetória de um veículo robótico terrestre de quatro rodas, *XIX Congresso Brasileiro de Automática (CBA 2012), Campina Grande, PB*.

- de Lemos, R. A., Sobral, G., Mirisola, L. G., Martins, R., Koyama, M. F., de Paiva, E. C., Bueno, S. S. and Antipolis-Méditerranée, I. S. (2017). Estratégia de navegação autônoma entre fileiras de cultivares baseada em laser, *XIII Simpósio Brasileiro de Automação Inteligente*.
- Fischler, M. A. and Bolles, R. C. (1981). Random sample consensus: a paradigm for model fitting with applications to image analysis and automated cartography, *Communications of the ACM* **24**(6): 381–395.
- Foley, J. A., Ramankutty, N., Brauman, K. A., Cassidy, E. S., Gerber, J. S., Johnston, M., Mueller, N. D., O’Connell, C., Ray, D. K., West, P. C. et al. (2011). Solutions for a cultivated planet, *Nature* **478**(7369): 337.
- Hiremath, S. A., Van Der Heijden, G. W., Van Evert, F. K., Stein, A. and Ter Braak, C. J. (2014). Laser range finder model for autonomous navigation of a robot in a maize field using a particle filter, *Computers and Electronics in Agriculture* **100**: 41–50.
- Nogueira, L. A. C. O., Koyama, M. F., Cordeiro, R. A., Ribeiro, A. M., Bueno, S. S. and Bueno, S. S. (2018). A miniaturized four-wheel robotic vehicle for autonomous driving research in off-road scenarios, *XXII Congresso Brasileiro de Automática*.
- Quigley, M., Conley, K., Gerkey, B. P., Faust, J., Foote, T., Leibs, J., Wheeler, R. and Ng, A. Y. (2009). Ros: an open-source robot operating system, *ICRA Workshop on Open Source Software*.
- Thanpattranon, P., Ahamed, T. and Takigawa, T. (2016). Navigation of autonomous tractor for orchards and plantations using a laser range finder: Automatic control of trailer position with tractor, *Biosystems Engineering* **147**: 90–103.
- Zuliani, M. (2009). Ransac for dummies, *Vision Research Lab, University of California, Santa Barbara*.